TWO-DIMENSIONAL COUPLED ELECTROSTATIC-MECHANICAL MODEL FOR RF MEMS SWITCHES

Ehab K. I. Hamad [1], Atef Z. Elsherbeni [2], Amr M. E. Safwat [3], and Abbas S. Omar [1]

[1] Chair of Microwave and Communications Engineering, University of Magdeburg, P.O. Box 4120, Magdeburg D-39106, Germany, http://iesk.et.uni-magdeburg.de/hf
[2] Center for Applied Electromagnetic Systems Research (CAESR), Electrical Engineering Department, The University of Mississippi, University, MS 38677, USA
[3] Electronics and Communications Engineering Department, Ain Shams University, Cairo 11517, Egypt

Ehamad@iesk.et.uni-magdeburg.de, atef@olemiss.edu, asafwat@ieee.org, and a.omar@ieee.org

***Abstract*:** Two-dimensional (2-D) coupled electrostatic-mechanical model of RF MEMS switches has been developed, in which the effect of residual stress due to the fabrication process and axial force resulting from the beam stretching have been taken into account. The electrostatic model is based on the application of the finite difference (FD) technique to quasi-static solution of a 2-D plane cut of the MEMS switch structure. The electrostatic model calculates the induced electrostatic force on the membrane due to the applied dc bias voltage. From the resulting electrostatic potential, the force distribution, the switch capacitance, and the beam deformation have been calculated. The computed pull down voltage for different structures agrees well with published data. The developed simulation program combines the electrostatic and mechanical analyses together and gives accurate results in short running time.

Keywords: 2-D MEMS modeling, Residual stress, Axial force, Coupled electro-mechanics, Shunt Capacitive MEMS switch, RF MEMS switches.

1. Introduction

RF MEMS switches are constructed using thin metal membrane, which can be electrostatically actuated using dc-bias voltage. Since they are designed on scales where the electrostatic force is capable to move or deform the membrane, 3-D or at least 2-D coupled electrostatic-mechanical model is needed for accurate prediction of the switch behavior. A simple one-dimensional lumped model, assumes that the shape of the deformed beam remains flat independent of its position has been presented earlier in [1]. This model is the simplest and most intuitive analytically, but its accuracy is very poor. Its purpose is for quick analysis to gain physical insight and understand overall behavior of the MEMS switches for RF and microwave application.

Two-dimensional electromechanical simulations assuming that the beam is made up of many horizontal-plate-to-ground-plane capacitors connected in parallel along the length of the beam have also been analyzed [2]. A three-dimensional quasi-static electro-mechanical model, as an application of CoSolve-EM software by combining the electromagnetic and mechanical simulators to determine the beam deformation, has been addressed in [3]. Although the latter gives very accurate results, the 3-D EM and mechanical simulators are sophisticated, expensive and require huge simulation time. An accurate solution, without sophistication, can easily be obtained using a two-dimensional mechanical model that is coupled to the electrostatic force distribution, and this is the core of this article.

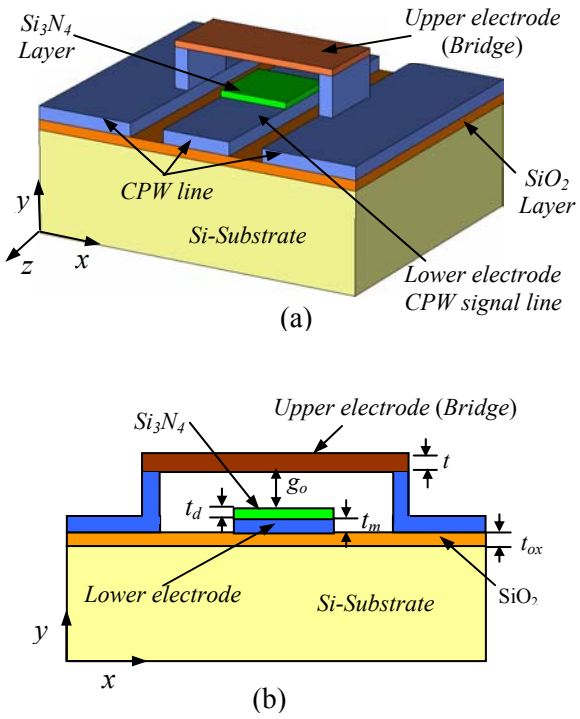

Fig. 1. Schematic diagram of fixed-fixed beam RF MEMS switch, (a) 3-D structure, (b) 2-D structure, *x*- *y* plane section.

The studied switch in this paper is electrostatically actuated and is doubly supported beam. A doubly supported or fixed-fixed beam RF MEMS switch usually consists of two parallel plates. One plate is fixed on the substrate, lower electrode, and the other is a movable membrane and is formed by a thin film metal that has good mechanical properties like Au or Cu prepared by electroplating process. A schematic diagram of a fixed-fixed beam shunt-capacitive RF MEMS switch is shown in Fig. 1. When a dc voltage is applied between the fixed and movable plates of the switch, the movable plate can move down onto the fixed electrode as a result of the electrostatic force induced due to the applied voltage. When the threshold (pull down) voltage is reached, the switch goes into the down state or OFF-state, and when no voltage is applied it goes into the up state or ON-state.

The purpose of this paper is to improve the algorithm, which has been presented elsewhere [4] to determine the deformation of the bridge in the shunt-capacitive RF MEMS switch as a function of the applied voltage. In [4] the effects of the residual and the axial stresses were not considered and also the electrostatic model was based on solving Laplace's equation. Most of the publications, either neglect the effect of the residual stress or the axial force or both of them [5]. To the authors' knowledge, the electrostatic force calculated in the literature is not in very accurate; some time the fringing field is neglected or used an approximate expression or the electrostatic force assumes uniformly distributed along the membrane [6-7]. Through this study the effect of the residual stress and the axial stress have been considered as well as the electrostatic force which has been calculated very accurately and as a non-uniform force distributed along the beam. The electrostatic model is based on Gauss's law applied to an inhomogeneous region with non-uniform discretization for accurate numerical simulation. The pull down voltage required to actuate the MEMS switch has been evaluated using the developed simulator. The main advantages of the proposed solution is that both electrostatic and mechanical models are combined in one simple Matlab-based program to determine the deformation of the switch's bridge, which is based on quasi-static solution in two-dimensions using the finite difference method (FDM). The choice of the fixed-fixed beam is based on the fact that this mechanical structure is the most common and the most basic to the surface-micro-machined MEMS structures. However, the developed simulation tool is easy to adapt to other configurations of MEMS structures.

2. Mathematical Algorithm

The starting point is to solve for the quasi-static potential in two-dimensions. Hence, the field distributions and the force induced on the membrane can be determined. Having the force distribution on the membrane makes it possible to activate the mechanical model in order to calculate the deformation in the membrane, which in turns alters the electrostatic field distribution. This cycle of electromechanical model is considered as one iteration. The program goes back and forth between the electrostatic and mechanical models until the difference between the maximum-deformation in the membrane in two successive iterations is less than 10^{-4} μm, which can be the program convergence criterion as defined by the user.

A. Electrostatic Model

The electrostatic model starts by generating the meshes with non-uniform grid sizes in both directions to get the minimum execution time with the highest possible accuracy. Next, Gauss's law is applied in the meshed region along with the finite difference technique to approximate the derivatives. The boundary conditions are $V = V_o$ on the lower electrode (CPW signal line) and $V = 0$ on the upper electrode (MEMS bridge) and the outer boundary. On the dielectric interface and at any node in the computational domain other than those on the electrodes, Gauss's law is applied.

The solution of the potential at the nodes of the grid inside the computational domain based on Gauss's law starts with

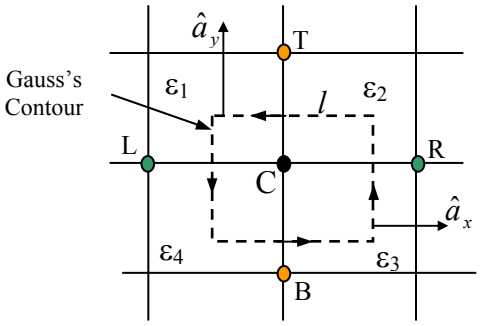

Fig. 2. A general voltage node C in the computational domain is surrounded by four voltage nodes, L, R, B, and T with four different media and the Gauss's contour.

$$-\oint_l \varepsilon \left(\frac{\partial V}{\partial x}\hat{a}_x + \frac{\partial V}{\partial y}\hat{a}_y \right) \bullet \hat{a}_n \, dl = 0 \qquad (1)$$

where the finite difference approximations translate this integral equation on the closed contour described in Fig. 2 to the following [8],

$$\frac{V_R-V_C}{x_R-x_C}\left[(y_T-y_C)\varepsilon_2+(y_C-y_B)\varepsilon_3\right]-\frac{V_C-V_L}{x_C-x_L}\left[(y_T-y_C)\varepsilon_1+(y_C-y_B)\varepsilon_4\right]$$
$$+\frac{V_T-V_C}{y_T-y_C}\left[(x_C-x_L)\varepsilon_1+(x_R-x_C)\varepsilon_2\right]-\frac{V_C-V_B}{y_C-y_B}\left[(x_R-x_C)\varepsilon_3+(x_C-x_L)\varepsilon_4\right]=0 \quad (2)$$

where the subscripts L, R, T, and B denote left, right, top, and bottom, respectively. This equation can be rearranged in the following general form:

$$V_C = C_R V_R + C_L V_L + C_T V_T + C_B V_B \quad (3)$$

where $C_R = C_o \dfrac{(y_T - y_C)\varepsilon_2 + (y_C - y_B)\varepsilon_3}{x_R - x_C}$,

$$C_L = C_o \frac{(y_T - y_C)\varepsilon_1 + (y_C - y_B)\varepsilon_4}{x_C - x_L},$$

$$C_T = C_o \frac{(x_R - x_C)\varepsilon_2 + (x_C - x_L)\varepsilon_1}{y_T - y_C},$$

$$C_B = C_o \frac{(x_R - x_C)\varepsilon_3 + (x_C - x_L)\varepsilon_4}{y_C - y_B},$$

and

$$C_o = \frac{1}{\left[\left(\frac{y_C-y_B}{x_R-x_C}+\frac{x_R-x_C}{y_C-y_B}\right)\varepsilon_3+\left(\frac{y_T-y_C}{x_R-x_C}+\frac{x_R-x_C}{y_T-y_C}\right)\varepsilon_2 + \left(\frac{y_C-y_B}{x_C-x_L}+\frac{x_C-x_L}{y_C-y_B}\right)\varepsilon_4+\left(\frac{y_T-y_C}{x_C-x_L}+\frac{x_C-x_L}{y_T-y_C}\right)\varepsilon_1\right]}.$$

Equation (3) has been solved using an iterative technique to find out the potential distribution everywhere in the computational domain. After solving for the potential distribution, the electric field vector can be calculated from the relation $\overline{E} = -\nabla V$ at every node, such that

$E_x = -\dfrac{\partial V}{\partial x}$ and $E_y = -\dfrac{\partial V}{\partial y}$.

Since we are using non-uniform grid, the potential can best be described at any arbitrary node using Lagrange's polynomials approximation, where

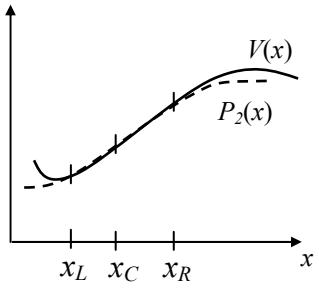

Fig. 3. Lagrange interpolation.

Lagrange's interpolating polynomial is described as:

$$V(x) \approx P_2(x) = \frac{(x-x_C)(x-x_R)}{(x_L-x_C)(x_L-x_R)}V(x_L) + \frac{(x-x_L)(x-x_R)}{(x_C-x_L)(x_C-x_R)}V(x_C) + \frac{(x-x_L)(x-x_C)}{(x_R-x_L)(x_R-x_C)}V(x_R)$$

where $P_2(x)$ is a second order degree polynomial which coincides with the exact function $V(x)$ at three nodes *L, R,* and *C* as shown in the Fig. 3.

Lagrange's interpolating polynomial is differentiated to obtain an approximation for the first order derivative and thus, the electric field vector components can be computed at any node *x* by

$$E_x(x) = -\frac{dV(x)}{dx} = -\frac{2x-x_C-x_R}{(x_L-x_C)(x_L-x_R)}V_L - \frac{2x-x_L-x_R}{(x_C-x_L)(x_C-x_R)}V_C - \frac{2x-x_L-x_C}{(x_R-x_L)(x_R-x_C)}V_R. \quad (4)$$

In the same way, the *y*-component at any node *y* can be computed.

The electrostatic model calculates the electrostatic force induced on the movable beam when a dc-bias voltage is applied between the upper and lower electrodes. When a dc-bias voltage is applied between the two plates, charges are induced on the membrane and opposite charges accumulate on the lower electrode. The induced charges per unit length ρ induced on the membrane are calculated using Gauss's law in two-dimensions as follows:

$$\rho = -\oint_l \varepsilon \frac{\partial V}{\partial n}\hat{n} \bullet \hat{a}_n dl \quad (5)$$

where *l* is a closed contour surrounding each subsection of the membrane as shown in Fig 4. Here $\hat{a}_n$ is the normal unit vector to the contour segments. By dividing the contour to four segments we obtain,

$$\rho = -\int_{right} \varepsilon(y)\frac{\partial V}{\partial x}dy - \int_{top} \varepsilon(x)\frac{\partial V}{\partial y}dx + \int_{left} \varepsilon(y)\frac{\partial V}{\partial x}dy + \int_{bottom} \varepsilon(x)\frac{\partial V}{\partial y}dx.$$

Assuming the field outside the metallic boundary and the voltage applied to the bridge to be zero, and the adjacent medium to the bridge surface is air with $\varepsilon_r = 1$. Thus, the accumulated charge per unit length distributed in the *z*-direction for any segment on the membrane centered at (x_c, y_c) can be calculated as:

$$\rho\ (x_C) = \varepsilon_o \frac{V_B}{y_C - y_B}\left[\frac{x_R - x_L}{2}\right].$$

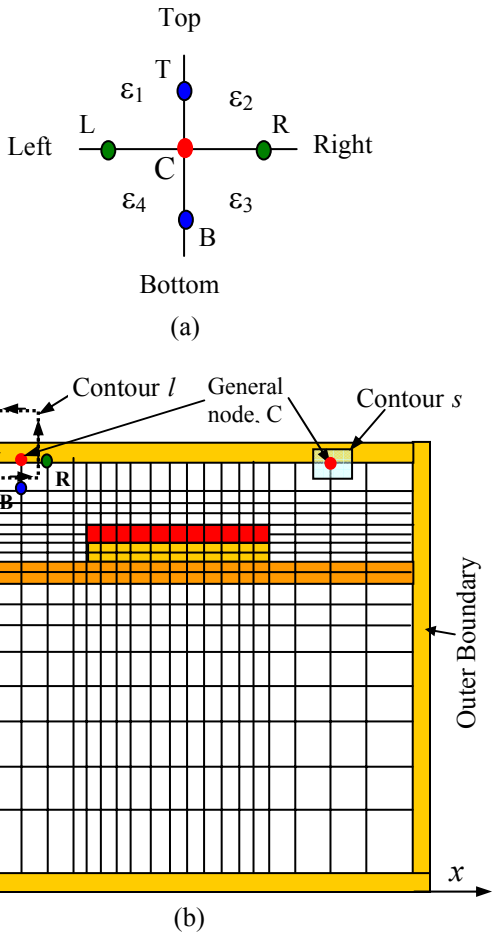

Fig. 4. (a) Notation of the potential and media properties in terms of the node coordinates for 2-D problem (b) Computational domain with the mesh distribution.

Dividing this equation by the segment length $(x_R - x_L)/2$ to find the charge density and multiplying it by b, the beam width, one can obtain the distributed charge per unit length on the bridge along the x-axis for any segment centered at x_c as:

$$\rho(x_C) = \varepsilon_o \frac{V_B}{y_C - y_B} b \ . \tag{6}$$

Having the electric field components, the electrostatic force induced on the bridge can be determined. The normal electrostatic force per unit length can be determined in terms of the storage energy U per unit length as: $f(x) = -dU(x,y)/dy$, where U is defined as $U = (1/2)\int_s \varepsilon\, E^2 dxdy$, and s is the surface contour shown in Fig. 4. Thus, $f(x) = (1/2)\int_l \varepsilon\, E^2 dx$ in Newton per unit length along the z-direction. Therefore, the amount of the electrostatic force induced on a certain segment of length Δx on the membrane is calculated by:

$$\Delta f(x) = (1/2)\,\varepsilon_o\, E^2(x, y \text{ at the bridge})\Delta x \ .$$

Dividing this equation by Δx to find the force density and multiplying it by the beam width b gives the distributed force per unit length in the x-direction induced on the bridge, thus at any arbitrary node x the distributed force per unit length is given as:

$$f(x) = \frac{b}{2}\varepsilon_o \left(E_x^2 + E_y^2\right). \tag{7}$$

In order to calculate the switch capacitance one needs to compute the total charge on the lower electrode then divide it by the applied voltage. Applying Gauss's law around the lower electrode as shown in Fig. 5. This leads to the following expression for the total enclosed charge.

$$\begin{aligned}\rho^{enc} = &-\sum_{right}\frac{V_R - V_C}{x_R - x_C}\left[\frac{\varepsilon_2(y_T - y_C) + \varepsilon_3(y_C - y_B)}{2}\right] \\ &-\sum_{top}\frac{V_T - V_C}{y_T - y_C}\left[\frac{\varepsilon_1(x_C - x_L) + \varepsilon_2(x_R - x_C)}{2}\right] \\ &+\sum_{left}\frac{V_C - V_L}{x_C - x_L}\left[\frac{\varepsilon_1(y_T - y_C) + \varepsilon_4(y_C - y_B)}{2}\right] \\ &+\sum_{bottom}\frac{V_C - V_B}{y_C - y_B}\left[\frac{\varepsilon_4(x_C - x_L) + \varepsilon_3(x_R - x_C)}{2}\right].\end{aligned} \tag{8}$$

The capacitance C per unit length is given next by $C = \rho^{enc}/V_o$, where V_o is the applied voltage between the lower and upper electrodes.

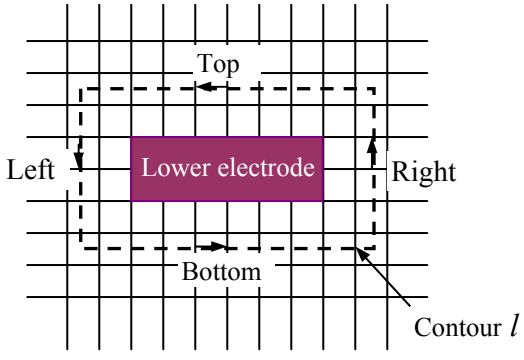

Fig. 5. Computation of the total charge accumulated on the lower electrode.

The accuracy of the results is completely dependant on the number of iterations, for this reason the program has been run for different numbers of iterations to get the optimal number. The maximum induced electrostatic force, the maximum deformation, and the switch capacitance in terms of the number of iterations are illustrated in Fig. 6-a, 6-b, and 6-c, respectively. The CPU time on a PC with Pentium IV, 1.4 GHz processor, and 2.0 GB RAM in terms of the number of iterations is plotted in Fig. 6-d as well. The maximum electrostatic force and the maximum deflection have been saturated after about 1000 iterations but the capacitance saturated after 2000 iterations. All subsequent data presented in this paper are generated on basis of 2000 iterations.

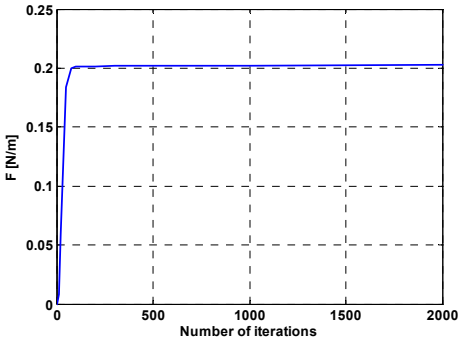

(a)

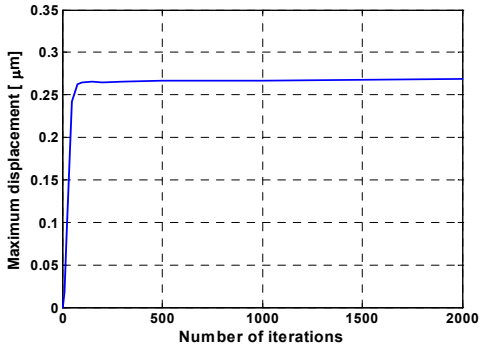

(b)

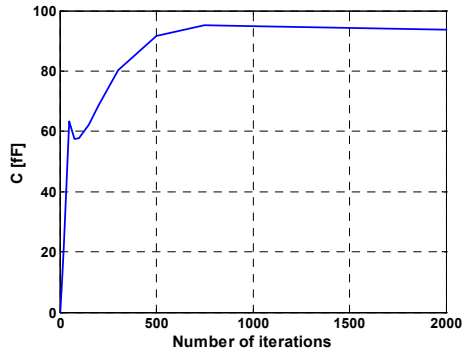

(c)

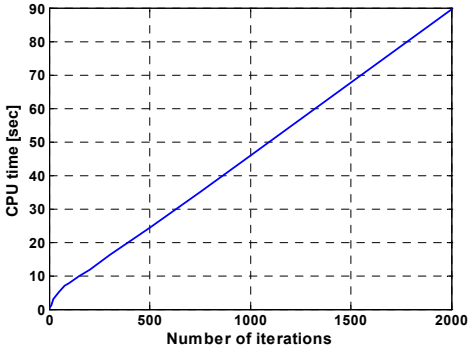

(d)

Fig. 6. (a) Maximum force vs. number of iterations (b) Maximum displacement vs. number of iterations (c) Capacitance vs. number of iterations (d) CPU time vs. number of iterations. The number of meshes are n_x = 72, n_y = 88 in the x and y directions, respectively. The mesh size is non-uniform in both x and y directions for more accurate solution, and it's minimized where fine geometrical details are present. dx_{min} = 2.8 (over the lower electrode region, where most of the field is confined), dx_{max} = 9 (at the end of the bridge, where approximately no field), dy_{min} = 0.0375 (in dielectric layer, the smallest thickness in the y-direction), and dy_{max} = 2.23 (at the bottom of substrate, where the field is decayed), all dimensions are in µm.

For the shunt-capacitive RF MEMS switch given in [1], where L (bridge length) = 300 µm, b (membrane width) = 80 µm, t (membrane thickness) = 2 µm, g_o (initial gap height) = 1.5 µm, W (lower electrode width) = 100 µm, t_m (lower electrode thickness) = 0.8 µm, t_{ox} (oxide layer thickness) = 0.4 µm, t_d (dielectric layer thickness) = 0.15 µm, the potential distribution after solving the static problem in the computation region is shown on Fig. 7. The charge distribution per unit length on the bridge based on Eq. (6) has been calculated with dc bias voltage of 30 Volts and plotted in Fig. 8-a. The corresponding distributed electrostatic force per unit length calculated using Eq. (7) is depicted in Fig. 8-b.

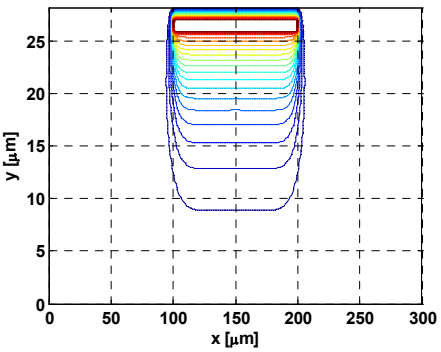

Fig. 7. Potential distribution in the computational domain with dc bias voltage of 30 Volts.

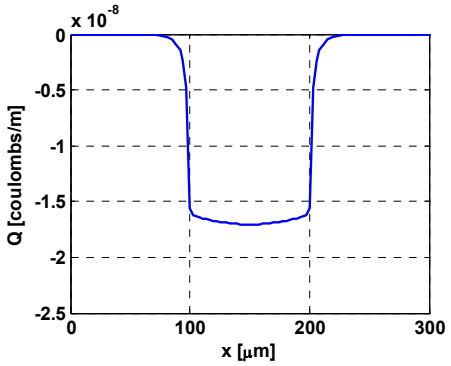

(a)

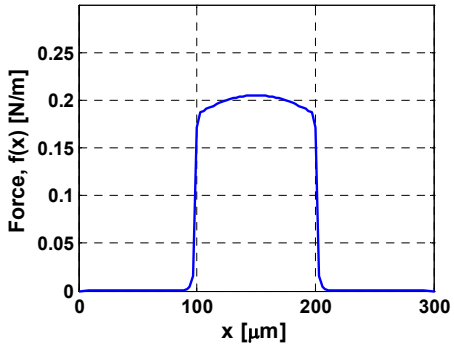

(b)

Fig. 8. (a) Charge distribution per unit length over the membrane with bias voltage of 30 Volts, (b) Force distribution per unit length induced on the membrane at bias voltage of 30 Volts.

B. Mechanical Model

Figures 1 and 9 show the fixed-fixed beam diagram and the load configuration, respectively. The step-up support in this beam has been approximated as a "fixed" boundary condition [9]. The transverse deflection of the movable beam $w(x)$ is governed by Euler-Bernoulli beam equation given in [10] as:

$$\hat{E}\tilde{I}\,\frac{\partial^4 w}{\partial x^4} - (T_r + T_a)\frac{\partial^2 w}{\partial x^2} = f(x) \qquad (9)$$

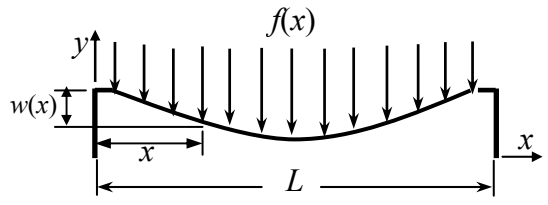

Fig. 9. Schematic diagram of the deformed electrostatic loaded double-supported beam.

where $f(x)$ is the distributed force per unit length (the beam here is electrostatically loaded and $f(x)$, which is the electrostatic force calculated from the electrostatic model couples the mechanical model and the electrostatic model). $w(x)$ is the beam displacement, $\hat{E} = E/(1\text{-}\nu^2)$ is the beam modulus where E is Young's modulus, ν is Poisson's ratio, $\tilde{I} = bt^3/12$ is the beam moment of inertia, t and b are the beam thickness and width, respectively. T_r is the residual force and is formulated by $T_r = \hat{\sigma}bt$, where $\hat{\sigma}$ is the residual stress which equals $\sigma_o(1-\nu)$ for the doubly supported beam, where σ_o is the biaxial residual stress. T_a is the axial force and is formulated by $T_a = \frac{\hat{E}bt}{2L}\int_0^L \left(\frac{dw}{dx}\right)^2 dx$.

To find the general solution of equation (9), it is more convenient to rewrite it in the form:

$$\frac{d^4 w}{dx^4} - k^2\frac{d^2 w}{dx^2} = F(x) \qquad (10)$$

where $k^2 = \frac{\hat{\sigma}bt}{\hat{E}\tilde{I}} + \frac{6b}{Lt^2}\int_0^L \left(\frac{dw}{dx}\right)^2 dx$, and $F(x) = \frac{f(x)}{\hat{E}\tilde{I}}$.

Equation (10) is a fourth order nonlinear, non-homogenous differential equation. If the axial force term $\frac{6b}{Lt^2}\int_0^L \left(\frac{dw}{dx}\right)^2 dx$ is neglected k will be constant equals to $\sqrt{\frac{\hat{\sigma}bt}{\hat{E}\tilde{I}}}$. Thus the 4th order differential equation will be linear but still non-homogenous. The general solution of a higher order non-homogenous linear differential equation can be found easily using the method of variation of parameters [11]. The general solution of this equation while, initially, assuming k is constant can be found by assuming the general solution of the homogenous equation of (10) to be in the form

$$w_c(x) = a_o + a_1 x + a_2 e^{kx} + a_3 e^{-kx}. \qquad (11)$$

Furthermore, by setting $w_o(x) = 1$, $w_1(x) = x$, $w_2(x) = e^{kx}$, and $w_3(x) = e^{-kx}$ in the last equation, one can use the method of variation of parameters for determining the particular solution $w_p(x)$ of Eq. (10) by determining four functions u_o, u_1, u_2, and u_3 such that

$$w_p(x) = u_o(x)\,w_o(x) + u_1(x)\,w_1(x) + u_2(x)\,w_2(x) + u_3(x)\,w_3(x). \qquad (12)$$

For these functions to be determined, four conditions must be specified. The Wronskian W of functions w_o, w_1, w_2, and w_3 is the determinant:

$$W(w_o, w_1, w_2, w_3) = \begin{bmatrix} w_o(x) & w_1(x) & w_2(x) & w_3(x) \\ w_o'(x) & w_1'(x) & w_2'(x) & w_3'(x) \\ w_o''(x) & w_1''(x) & w_2''(x) & w_3''(x) \\ w_o'''(x) & w_1'''(x) & w_2'''(x) & w_3'''(x) \end{bmatrix}$$

while $u_k' = \frac{W_k}{W}$, where W_k is the determinant obtained by replacing the k^{th} column of the Wronskian by the column consisting of the elements $(0,0,0, F(x))$. Simple integration can be used to obtain $u_o(x)$, $u_1(x)$, $u_2(x)$, and $u_3(x)$, while substitution in Eq. (12) yields the particular solution

$$u_o(x) = \frac{1}{a_o k^2}\int xF(x)dx\,,\; u_1(x) = -\frac{1}{a_1 k^2}\int F(x)dx\,,$$

$$u_2(x) = \frac{1}{2a_2 k^3}\int e^{-kx}F(x)dx,\; u_3(x) = -\frac{1}{2a_3 k^3}\int e^{kx}F(x)dx$$

with

$$w_p(x) = \frac{1}{k^2}\int xF(x)dx - \frac{x}{k^2}\int F(x)dx + \frac{e^{kx}}{2k^3}\int e^{-kx}F(x)dx - \frac{e^{-kx}}{2k^3}\int e^{kx}F(x)dx.$$

Thus, the general solution of $w(x)$ equals $w_c(x) + w_p(x)$, which can be found as:

$$w(x) = a_o + a_1 x + a_2 e^{kx} + a_3 e^{-kx} + \frac{1}{k^2}\int_0^x \lambda F(\lambda)\,d\lambda - \frac{x}{k^2}\int_0^x F(\lambda)\,d\lambda + \frac{e^{kx}}{2k^3}\int_0^x e^{-k\lambda}F(\lambda)\,d\lambda - \frac{e^{-kx}}{2k^3}\int_0^x e^{k\lambda}F(\lambda)\,d\lambda \tag{13}$$

where a_0, a_1, a_2, and a_3 are constants to be determined by applying the boundary conditions $w(0) = 0 = w'(0)$ and $w(L) = 0 = w'(L)$, with assumed clamped-clamped beam. The coefficients a_0, a_1, a_2, and a_3 can be determined from the following matrix equation:

$$\begin{bmatrix} a_0 \\ a_1 \\ a_2 \\ a_3 \end{bmatrix} = \begin{bmatrix} 1 & 0 & 1 & 1 \\ 0 & 1 & \mathrm{k} & -\mathrm{k} \\ 0 & \mathrm{L} & \mathrm{e}^{\mathrm{kL}} & \mathrm{e}^{-\mathrm{kL}} \\ 0 & 1 & \mathrm{ke}^{\mathrm{kL}} & -\mathrm{ke}^{-\mathrm{kL}} \end{bmatrix}^{-1} \begin{bmatrix} 0 \\ 0 \\ b_1 \\ b_2 \end{bmatrix} \tag{14}$$

where

$$b_1 = -\frac{1}{k^2}\int_0^L \lambda F(\lambda)\,d\lambda + \frac{L}{k^2}\int_0^L F(\lambda)\,d\lambda - \frac{e^{kL}}{2k^3}\int_0^L e^{-k\lambda}F(\lambda)\,d\lambda + \frac{e^{-kL}}{2k^3}\int_0^L e^{k\lambda}F(\lambda)\,d\lambda$$

and

$$b_2 = \frac{1}{k^2}\int_0^L F(\lambda)\,d\lambda - \frac{e^{kL}}{2k^2}\int_0^L e^{-k\lambda}F(\lambda)\,d\lambda - \frac{e^{-kL}}{2k^2}\int_0^L e^{k\lambda}F(\lambda)\,d\lambda\,.$$

The integrals for the b coefficients are all finite and are computed numerically.

Now to include the axial force in this analysis, we use the resulting $w(x)$ to determine the axial force term $\frac{6b}{Lt^2}\int_0^L \left(\frac{dw}{dx}\right)^2 dx$ and then calculate the new value of k and substitute back in Eq. (13) using the new values of the a coefficients calculated from Eq. (14) to determine the new $w(x)$. Repeating this process until the difference between two successive iterations for k is within pre-determined value. In our procedure the error was set to be lower than 10^{-10} m^{-1}.

C. Coupled Electrostatic-Mechanical Model

When a dc voltage is applied to the un-actuated MEMS switch shown in Fig. 1, it induces charges on the surface of the membrane that in turn induce a normal electrostatic force over the membrane, as given by Eq. (7). The electrostatic force causes the beam to deform. Such deformation will lead to a reorganization of the surface charges. The force distribution on the beam is schematically shown in Fig. 6-b. If this reorganization of charges is large enough to cause further deformation, the process is necessary to resolve the electrostatic problem to recalculate the new induced electrostatic force and this is considered as a coupled electro-mechanical behavior. The new electrostatic force is used by the mechanical model to determine the new transverse deflection. Going back and forth between these two models is carried out until the difference between two successive iterations for the transverse deflection is in a pre-determined specified error. In our procedure the error has been set to be less than 10^{-10} m.

For MEMS analysis, it is usually assumed that the pull down occurs when the microstructure deflects down to $(2/3)g_o$, where g_o is the initial gap height. This is considered the unstable mechanical position of the bridge. Hence the back and forth switching between the electric and mechanical models converges as long as the switch works in the mechanical stability region other-wise it may diverge. Therefore, the iterations is stopped when the maximum deflection is greater than or equal $(2/3)g_o$, which corresponds to the pull down voltage for the MEMS switch.

3. Results and Discussion

To validate the obtained numerical results, we compare the results of the maximum deflection calculated using our approach to those reported in [1] with the parameters shown in Fig. 1 for doubly supported beam of the dimensions given in section 2-A. The silicon-nitride Si_3N_4 and silicon-oxide SiO_2 dielectric layers have relative dielectric constants of 7.6 and 3.9, respectively. The Young's modulus E amounts to 80 GPa, the Poison's ratio ν is equal to 0.42, and the biaxial residual stress σ_o is equal to 20 MPa.

The computed maximum displacement and the gap capacitance as functions of the number of iterations are shown in Fig. 10. The steady state condition has been reached after 9 iterations between the electrostatic and mechanical solutions. The iterations stopped when the error in the maximum deflection curve falls below a tolerance value (here given as 10^{-4} μm) or the maximum deflection increases than $(2/3)g_o$, which means the applied voltage is greater than or equals the pull down voltage. Figure 11-a illustrates the gap height versus applied voltage, while Fig. 11-b illustrates the gap capacitance versus applied voltage. The shape of the bridge as a function of applied voltage is investigated in Fig. 12. The computed pull down voltage amounts to 35 Volts while the experimental value for similar configuration is usually reported to be in the range of 30 Volts. The computed up-position capacitance of the MEMS switch is 85 fF while the experimental value is 70 fF. The theoretical results are very close to the experimental values reported in the literatures.

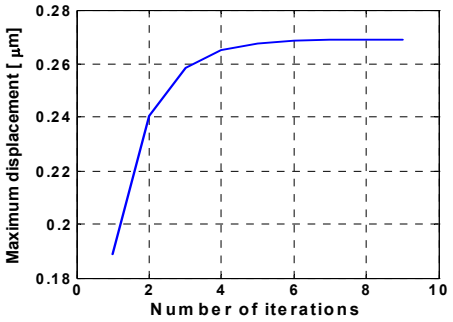

Fig. 10. (a) Maximum displacement and (b) Switch capacitance as a function of the number of iterations of going and back between the electrostatic and mechanical models at dc bias voltage of 30 Volts.

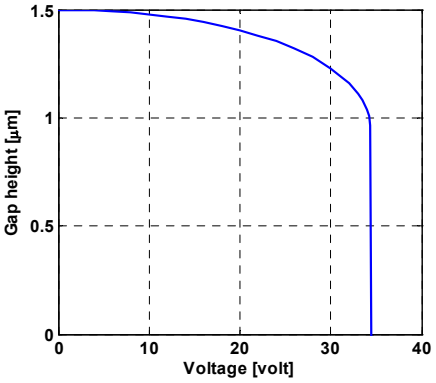

Fig. 11-a. Gap height versus applied voltage.

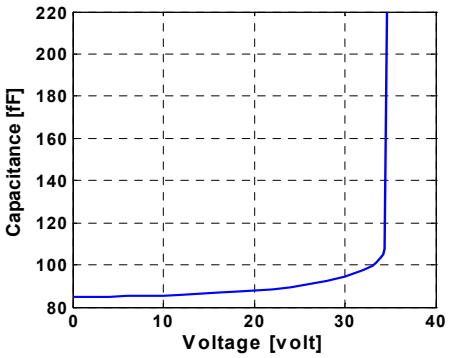

Fig. 11-b. Capacitance versus applied voltage.

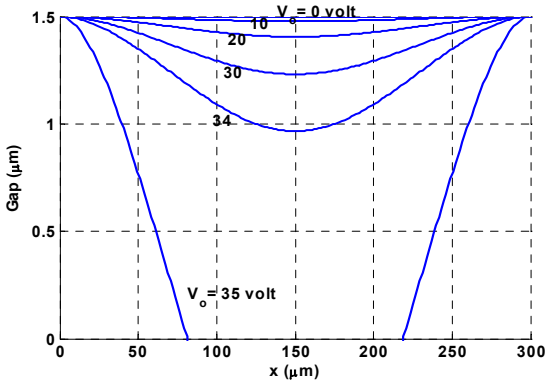

Fig. 12. Shape of the membrane as a function of applied voltage.

4. Conclusion

In this paper, a novel two-dimensional coupled electro-mechanical model has been developed, where the axial and residual stresses are taken into consideration. A Simulation program is developed to

determine the deformation of the bridge in RF MEMS switches as a function of the applied voltage. The electrostatic model is based on solving Gauss's law in a two-dimensional Cartesian coordinates system using the central difference approximation for the derivatives. An iterative procedure is implemented for the solution of the potential distribution. The algorithm is very efficient to determine the pull down voltage of the shunt-capacitive MEMS switch. However, it can be used for other types of MEMS switches like series or shunt configuration, capacitive or resistive contact as well.

The developed algorithm and the program presented are capable to determine the bridge deformation, pull-in voltage and to investigate the effect of source fluctuations on the switch performance efficiently. Due to its numerical efficiency and small CPU time requirement, the proposed technique can be integrated easily in computer-aided design tools for MEMS switches.

References

[1] J. B. Muldavin, G. M. Rebeiz, "High-Isolation CPW MEMS Shunt Switches-Part 1: Modeling", *IEEE Transaction on Microwave Theory and Techniques*, Vol. 48, No. 6, pp. 1045-1052, June 2000.

[2] E. K. Chan, K. Garikipati, and R. W. Dutton, "Characterization of Contact Electromechanics Through Capacitance-Voltage Measurements and Simulations", *IEEE Journal of MEMS*, Vol. 8. No. 2, pp. 208-217, June 1999.

[3] J. R. Gilbert, R. Legtenberg, and S. D. Senturia, "3D coupled electro-mechanics for MEMS: application of CoSolve-EM," Proceeding of *Int. IEEE MEMS Conference*, pp. 122-127, 1995.

[4] E. K. I. Hamad, A. M. E. Safwat, and A. S. Omar, "2-D Coupled Electrostatic-Mechanical Model for Shunt-Capacitive MEMS Switch Based on Matlab Program," Proceeding of *the IEEE/ACES International Conference*, Honolulu, Hawaii, USA, April 2005.

[5] Q. Meng, M. Mehregany, and R. L. Mullen, "Theoretical Modeling of Microfabricated Beams with Elastically Restrained Supports", *IEEE Journal of MEMS*, Vol. 2, pp. 128-137, Sept. 1993.

[6] B. Choi and E. G. Lovell, "Improved Analysis of Microbeams under Mechanical and Electrostatic Loads", *Journal of Micromech Microeng*, Vol. 7, pp. 24–29, 1997.

[7] L. X. Zhang, Y.-P. Zhao, "Electromechanical Model of RF MEMS Switches", *Microsystem Technologies* 9, pp. 420–426, 2003.

[8] A. Z. Elsherbeni, "The Finite Difference Technique for Electromagnetic Applications", Electrical Engineering Department, The University of Mississippi, University, MS 38677, USA, May 2005.

[9] P. Osterberg, H. Yie, X. Cai, J. White, and S. Senduria "Self-Consistent Simulation and Modeling of Electrostatically Deformed Diaphragms", Proceeding of *Int. IEEE MEMS Conference*, Oiso, Japan, pp. 28-32, January 1994.

[10] S. P. Timoshenko and J. M. Gere "Theory of Elastic Stability", *McGraw-Hill Inc.,* New York, 2nd ED., 1961.

[11] W. E. Boyce and R. C. Diprima, "Elementary Differential Equations and Boundary Value Problems", *John Wiley & Sons, Inc*. New York, 6th ED. 1997.

Ehab K. I. Hamad was born in Assiut, Egypt in 1970. He received his B.Sc. in Electrical Engineering and M.Sc. in Electronics and Communications Engineering from Assiut University, Assiut, Egypt, in 1994 and 1999, respectively. From 1999 to 2001 he was a Teaching/ Research Assistant in Electrical Engineering Department, Aswan Faculty of Engineering, South Valley University, Aswan, Egypt. He is currently working toward the Ph.D. degree in Microwave and Communications Engineering at Otto-von-Guericke-University Magdeburg, Magdeburg, Germany.

Mr. Hamad has jointed the Chair of Microwave and Communication Engineering, University of Magdeburg since 2001. His research interests include MEMS analysis, design, modeling, and fabrication with special interest in RF MEMS switches and filters for RF and microwave applications. He is interested also in planar microwave circuits for wireless applications.

Atef Z. Elsherbeni received an honor B.Sc. degree in Electronics and Communications, an honor B.Sc. degree in Applied Physics, and a M.Eng. degree in Electrical Engineering, all from Cairo University, Cairo, Egypt, in 1976, 1979, and 1982, respectively, and a Ph.D. degree in Electrical Engineering from Manitoba University, Winnipeg,

Manitoba, Canada, in 1987. He was a Research Assistant with the Faculty of Engineering at Cairo University from 1976 to 1982, and from 1983 to 1986 at the Electrical Engineering Department, Manitoba University. He was a part time Software and System Design Engineer from March 1980 to December 1982 at the Automated Data System Center, Cairo, Egypt. From January to August 1987, he was a Post Doctoral Fellow at Manitoba University. Dr. Elsherbeni joined the faculty at the University of Mississippi in August 1987 as an Assistant Professor of Electrical Engineering. He advanced to the rank of Associate Professor on July 1991, and to the rank of Professor on July 1997. He became the director of The School of Engineering CAD Lab at the University of Mississippi on August 2002, and the associate director of The Center for Applied Electromagnetic Systems Research (CAESR) at The University of Mississippi on August 2002. He was appointed as Adjunct Professor, at The Department of Electrical Engineering and Computer Science of the L.C. Smith College of Engineering and Computer Science at Syracuse University on January 2004. He spent a sabbatical term in 1996 at the Electrical Engineering Department, University of California at Los Angeles (UCLA) and was a visiting Professor at Magdeburg University during the summer of 2004.

Dr. Elsherbeni received The Mississippi Academy of Science 2003 Outstanding Contribution to Science Award, The 2002 IEEE Region 3 Outstanding Engineering Educator Award, The 2002 School of Engineering Outstanding Engineering Faculty Member of the Year Award, the 2001 Applied Computational Electromagnetic Society (ACES) Exemplary Service Award for leadership and contributions as Electronic Publishing Managing Editor 1999-2001, the 2001 Researcher/Scholar of the year award in the Department of Electrical Engineering, The University of Mississippi, and the 1996 Outstanding Engineering Educator of the IEEE Memphis Section.

Dr. Elsherbeni has conducted research in several areas such as: scattering and diffraction by dielectric and metal objects, inverse scattering, finite difference time domain analysis of passive and active microwave devices, field visualization and software development for EM education, dielectric resonators, interactions of electromagnetic waves with human body, and development of sensors for soil moisture and for monitoring of airports noise levels, air quality including haze and humidity, reflector antennas and antenna arrays, and analysis and design of printed antennas for radars and communication systems. His recent research has been on the application of numerical techniques to microstrip and planar transmission lines, antenna measurements, and antenna design for radar and personal communication systems. He has published 82 technical journal articles and 17 book chapters on applied electromagnetics, antenna design, and microwave subjects, and contributed to 230 professional presentations and offered 16 short courses and 17 invited seminars. He is the coauthor of the book entitled "MATLAB Simulations for Radar Systems Design", CRC Press, 2003 and the main author of the chapters "*Handheld Antennas"* and "*The Finite Difference Time Domain Technique for Microstrip Antennas"* in Handbook of Antennas in Wireless Communications, CRC Press, 2001.

Dr. Elsherbeni is a senior member of the Institute of Electrical and Electronics Engineers (IEEE). He is the Editor-in-Chief for the Applied Computational Electromagnetic Society (ACES) Journal, an Associate Editor to the Radio Science Journal, and the electronic publishing managing editor of ACES. He serves on the editorial board of the Book Series on Progress in Electromagnetic Research, the Electromagnetic Waves and Applications Journal, and the Computer Applications in Engineering Education Journal. He was the Chair of the Engineering and Physics Division of the Mississippi Academy of Science and the Chair of the Educational Activity Committee for the IEEE Region 3 Section. Dr. Elsherbeni's home page can be found at http://www.ee.olemiss.edu/atef and his email address is Elsherbeni@ieee.org.

Amr M. E. Safwat was born in Cairo, Egypt in May 1970. He received the B. S. and the M.S. from Ain Shams University, Cairo, Egypt in 1993 and 1996 respectively and the Ph.D. from University of Maryland, College park in 2001. All are in Electrical Engineering.

He was a Research and Teaching Assistant at Ain Shams University from 1993-1997. From 1997- 2001 he was a Research Assistant in Laboratory for Physical Sciences, University of Maryland. From Aug. 2001 to Aug. 2002 he was with Cascade Microtech, Inc, where he co-developed the infinity probes and the on wafer differential calibration standards. In Aug. 2002, he joined the Electronics and Communications Engineering Department, Ain Shams University as Assistant Professor. He was a Researcher/ Visiting Professor in the Institute Polytechnique de Grenoble (INPG) France in 1994 and in the Otto-von-Guericke-University Magdeburg Germany in 2004. His research interests include microwave opt-electronic oscillator,

high-speed photo-detectors, on-wafer probing and microwave integrated circuits.

Abbas S. Omar received the B.Sc., M.Sc. and Doktor-Ing. degrees in Electrical Engineering in 1978, 1982 and 1986, respectively. He has been Professor of Electrical Engineering since 1990 and head of the Chair of Microwave and Communication Engineering at the University of Magdeburg, Germany since 1998. He authored and co-authored more then 200 technical papers extending over a wide spectrum of research areas. Recently, he directed his search activities to the solution of inverse problems related to remote sensing and microwave tomography. His current research fields cover the areas of remote sensing and microwave imaging, in- and outdoor wireless communication, wideband satellite and mobile communication, electromagnetic bullets and their applications to secure, low power, wideband communications and subsurface tomography, stochastical electromagnetics and their meteorological, environmental and biomedical applications, field theoretical modeling of microwave systems and components, microwave measurements and sub-millimeter wave signal generation and processing.

Dr. Omar is member of the Technical Program Committee of IEEE MTT-S Symposium and member of the editorial board of IEEE Trans. MTT, IEEE Trans. AP, IEEE Trans. MI, IEEE Microwave and Wireless Components Letters, Proceeding IEE, Electronics Letters, Journal of Electromagnetics, Canadian Journal of Physics and Radio Science.